ORIGINAL ARTICLE

Injectable vaginal bio-adhesive gel activated by hard nano ceramic particles: *in vitro* and *in vivo* properties

Gel bioadhesivo vaginal inyectable activado por partículas nanocerámicas duras: propiedades in vitro e in vivo

Zeynep D. Şahin-Inan[1], Kerim E. Öksüz[2,3], Begüm Kurt[4], Ceylan Hepokur[5], and Yener Ünal[6]*

[1]Department of Histology Embryology, Faculty of Medicine, Sivas Cumhuriyet University; [2]Department of Metallurgical and Materials Engineering, Faculty of Engineering, Sivas Cumhuriyet University; [3]Department of Bioengineering, Institute of Science and Technology, Sivas Cumhuriyet University; [4]Department of Obstetrics and Gynecology, Faculty of Medicine, Sivas Cumhuriyet University; [5]Department of Basic Pharmaceutical Sciences, Biochemistry, Faculty of Pharmacy, Sivas Cumhuriyet University; [6]Department of Statistics and Computer Sciences, Faculty of Science, Sivas Cumhuriyet University. Sivas, Türkiye

Abstract

Objective: *This study aimed to synthesize, characterize, and evaluate the histopathological and biochemical efficacy of vaginal gels (VGs) in healing lacerations resulting from vaginal trauma. The bioadhesive gel containing nanoparticles (n-HAp) represents a novel application in this field.* **Methods:** *VGs were synthesized using n-HAp and characterized by field emission scanning electron microscopy (FE-SEM) and X-ray diffraction (XRD). High-resolution FE-SEM images confirmed the presence of n-HAp, while XRD verified its structural properties. Four experimental groups were established: Control, Sham, VG, and VG/n-HAp. Tissue and blood samples were collected on days 7, 14, and 21.* **Results:** *Biochemical parameters such as tumor necrosis factor-alpha (TNF-), interleukin-1 (IL-1), and vascular endothelial growth factor (VEGF) were evaluated in serum samples. Histological evaluations included inflammation, granulation tissue formation, collagen and reticular fiber density, re-epithelialization, and neovascularization. The VG/n-HAp group exhibited significantly faster healing and more pronounced inflammatory responses over time compared to the other groups.* **Conclusion:** *Overall, the addition of n-HAp to VGs accelerated both biochemical and histopathological recovery in a rat vaginal wound healing model.*

Keywords: *Bioadhesive gel. Vaginal wound model. Tissue repair. Nanomaterial.*

Resumen

Objetivo: *Este estudio tuvo como objetivo sintetizar, caracterizar y evaluar la eficacia histopatológica y bioquímica de los geles vaginales (GV) en la cicatrización de laceraciones causadas por traumatismos vaginales. El gel bioadhesivo que contiene nanopartículas (n-HAp) representa una aplicación novedosa en este campo.* **Métodos:** *Los GV fueron sintetizados a partir de n-HAp y caracterizados mediante microscopía electrónica de barrido de emisión de campo (FE-SEM) y difracción de rayos X (XRD). Las imágenes de alta resolución obtenidas por FE-SEM confirmaron la presencia de n-HAp, y las pruebas de XRD validaron sus propiedades estructurales. Se establecieron cuatro grupos experimentales: Control, Sham, GV y GV/n-HAp. Se recolectaron muestras de tejido y sangre en los días 7, 14 y 21.* **Resultados:** *Se evaluaron parámetros bioquímicos como el factor de necrosis tumoral alfa (TNF-), la interleucina-1 (IL-1) y el factor de crecimiento endotelial vascular (VEGF) en muestras séricas. Las evaluaciones histológicas incluyeron inflamación, formación de tejido de granulación, densidad de fibras colágenas y reticulares, reepitelización y neovascularización. El grupo GV/n-HAp mostró una cicatrización significativamente más rápida y procesos inflamatorios más marcados a lo largo del tiempo en comparación con los demás grupos.*

***Correspondence:**
Zeynep D. Şahin İnan
E-mail: zinan@cumhuriyet.edu.tr

Date of reception: 17-09-2024
Date of acceptance: 02-12-2024
DOI: 10.24875/CIRU.24000502

Cir Cir. 2025;93(4):395-410
Contents available at PubMed
www.cirugiaycirujanos.com

Conclusiones: *En general, la adición de n-HAp a los GV aceleró la recuperación tanto bioquímica como histopatológica en un modelo de cicatrización de heridas vaginales en ratas.*

Palabras clave: *Gel bioadhesivo. Modelo de herida vaginal. Reparación tisular. Nano material.*

Introduction

Vaginal and perineal trauma, particularly during vaginal childbirth, represents a significant clinical challenge affecting approximately 75% of women. These injuries result in both short-term and long-term morbidity[1]. The impact of such trauma on women's quality of life can be substantial, potentially disrupting newborn care and breastfeeding. In addition, postpartum perineal pain, dyspareunia, and esthetic concerns may lead women to avoid normal vaginal delivery and opt for elective cesarean sections. The increasing rates of cesarean deliveries raise concerns in obstetric care, as high cesarean rates are considered indicators of poor quality. Health-care providers should strive to minimize the potential short- and long-term effects of perineal trauma and pain through evidence-based interventions[2].

Perineal lacerations can lead to pelvic pain, decreased sexual quality of life, and psychological trauma. Approximately 30% of women experience discomfort within the first 2 weeks after childbirth, and maternal pain and discomfort are common in first- and second-degree perineal tears[3].

Novel therapeutic approaches are needed to contribute to perineal wound healing, enhance tissue strength, and facilitate mothers' quicker return to normal activities.

Bioadhesive gels, with their ability to adhere to tissue surfaces, provide sustained drug release and support tissue regeneration, and have gained attention as potential therapeutic agents for wound healing. Nano-hydroxyapatite (n-HAp)-based bioadhesive gels show promise in various medical applications, including bone repair and tissue engineering. However, their efficacy in vaginal wound healing remains relatively unexplored[4-7].

In this study, we investigate the histopathological and biochemical effects of a novel bioadhesive gel prepared with nano hydroxyapatite particles in a rat model of vaginal lacerations. Our goal is to assess its potential as an adjunctive therapy for enhancing wound healing in vaginal trauma.

Furthermore, the usability of nano ceramic particles, which are frequently used in hard tissue applications, in soft and delicate tissue applications has been investigated in detail for the 1st time in this study.

We hypothesize that the incorporation of n-HAp into the gel formulation will accelerate the healing process, reduce inflammation, and improve tissue repair. Understanding the mechanisms underlying the effects of n-HAp-based bioadhesive gels on vaginal wound healing may provide valuable insights for clinical applications. By elucidating the cellular and molecular processes involved, we aim to contribute to the development of novel therapeutic strategies for managing vaginal trauma and improving patient outcomes.

Methods

Chemicals and reagents

Nanoparticles and vaginal gels (VGs) synthesis were performed with analytical grade, sodium hypochlorite (NaClO), EtOH, (CH_3CH_2OH, 190 proof, ACS spectrophotometric grade, 95.0% non-denatured ethanol), *isopropanol* (propan-2-ol, 70% in H_2O, $CH_3CH(OH)CH_3$), carboxymethyl cellulose sodium (CM-cellulose; CMC-Na, Viscosity: 1000-1400 mpa.s, standard deviation [SD] = 1.2), glycerol (Pharmaceutical-grade), acetic acid, (CH_2COOH, glacial, ReagentPlus®, ≥ 99%) and ammonium polyacrylate dispersing agent (DARVAN 821-A) were purchased from Sigma-Aldrich (St. Louis, USA). The Milli-Q50 SP Reagent Water System (Millipore Corporation, MA, USA) was employed to produce ultrapure water, which was subsequently used in the sample preparation process. All other *in vitro* and *in vivo* experimental supplies and reagents were of analytical grade and were purchased from Merck KGaA (Darmstadt, Germany), Thermo Fisher Scientific (Massachusetts, USA), and Bayer AG (Leverkusen, Germany).

Production of hydroxyapatite nanoparticles (n-HAp)

As per our previous research[8,9]. n-HAp was synthesized from natural bovine bones (femur) through a detailed method outlined below. Initially, freshly

collected bone segments were thoroughly cleansed and subjected to six cycles of boiling in dH_2O. To remove any residual fats, they were then degreased using 70% ethanol (EtOH). Subsequently, the bone pieces were immersed in a solution of NaClO (30% v/v) and left to dry for a minimum of 48 h before further processing. The dried bone segments underwent a calcination process at a temperature of 850°C, with a gradual heating rate of 5°C/min, and were maintained at this temperature for 4 h in the presence of air to ensure the elimination of any prions, such as Creutzfeldt-Jakob disease or Bovine Spongiform Encephalopathy. Following calcination, the bovine femoral bone parts were finely crushed into small pieces and then subjected to planetary ball milling using the Fritsch Planetary Micro Mill Pulverisette 7 premium line from Germany. This milling process was carried out in isopropyl alcohol using ZrO_2 balls at a speed of 300 cycles/min for a duration of 144 h, maintaining a ball-to-powder ratio of 10:1. Subsequently, the milled powder samples were dried in a pyrex pan. Ultimately, the resultant natural hydroxyapatite nanoparticles (n-HAp) were stored at RT in a desiccator for further use[10,11]. Figure 1 shows the experimental steps followed in obtaining n-HAp. This rigorous method ensures the production of high-quality n-HAp from bovine bones, providing valuable biomaterials for various biomedical applications.

Pharmaceutical compositions of n-HAp loaded bioadhesive VGs

Hydrogels, which are composed of gel formers, have been the subject of previous investigations and applications for drug delivery or administering other injectable substances. While certain hydrogels have demonstrated promising characteristics, such as degrading and dissipating from the injection site within a few days, there remain challenges to address. Some existing hydrogels lack the desired cohesiveness, resulting in dispersion after injection. In addition, certain hydrogels tend to degrade relatively rapidly when introduced into living organisms. In cases where these hydrogels incorporate hard ceramic particles to facilitate soft and/or hard tissue augmentation, the presence of bioceramic particles in the hydrogel can lead to ion release and potential contamination[12,13]. To achieve optimal outcomes, it becomes crucial to mitigate these concerns and ensure the bioceramic particles' influence on the hydrogel remains adequately controlled. Consequently, further research and development are needed to improve the performance and biocompatibility of hydrogels or biomaterials when combined with hard ceramic particles for tissue augmentation purposes[14,15]. By addressing these challenges, we can advance the potential of such hydrogel-based systems for various medical applications. A homogeneous aqueous solution was prepared using distilled water (dH_2O) by adding 0.5% v/v of acetic acid (CH_2COOH) to 100 mL at RT with vigorous stirring (pH ~4.8-5.1). Subsequently, 1.5% w/v of CMC-Na and 0.75% w/v of SA powder were carefully introduced into the solution and stirred at 37°C until complete solubilization was achieved. To facilitate the carboxymethylation reaction, the reagents were combined, and 6.5% v/v of glycerol was slowly added to the mixture, resulting in the formation of a uniform sticky solution. The reaction was allowed to proceed at 37°C for 6 h in a water bath to ensure complete carboxymethylation[16].

To prepare the n-HAp-loaded bioadhesive VG, the prepared n-HAp was first dispersed in 1 mL of dH_2O using an optimized quantity of ammonium polyacrylate solution (0.5% v/v), which served as a dispersing agent (DARVAN821-A). This dispersion was achieved through 15 min of sonication using an ultrasonic homogenizer (SONICS, VCX/750, Ultrasonic processors, Newtown, U.S.A.) at a concentration of 0.75% (w/v). The choice of 0.75 wt.% concentration was primarily to prevent clustering or agglomeration of nanoparticles, as observed at higher concentrations. After surface modification of the n-HAp with ammonium polyacrylate, the n-HAp solution was blended with the gel solution using low-shear mixing for 1 h to create the n-Hap-loaded bioadhesive VG/nHAp polymer solutions, maintaining a pH of approximately 4.5[17]. Subsequently, the prepared solutions were sealed and kept at RT for 24 h to allow the hydrolysis and polycondensation reactions to take place, leading to the completion of the gelation process. The same experimental procedure was applied to prepare the unloaded n-HAp gel (VG). Both resulting bioadhesive VGs were subjected to gamma irradiation in 10 cc syringes to achieve both sterilization and cross-linking, ensuring their sterility and stability[18]. The prepared calcium phosphate salts have been adjusted to a pH of 4.5 to ensure that the healthy vaginal environment falls within the pH range of 3.5-4.5[17].

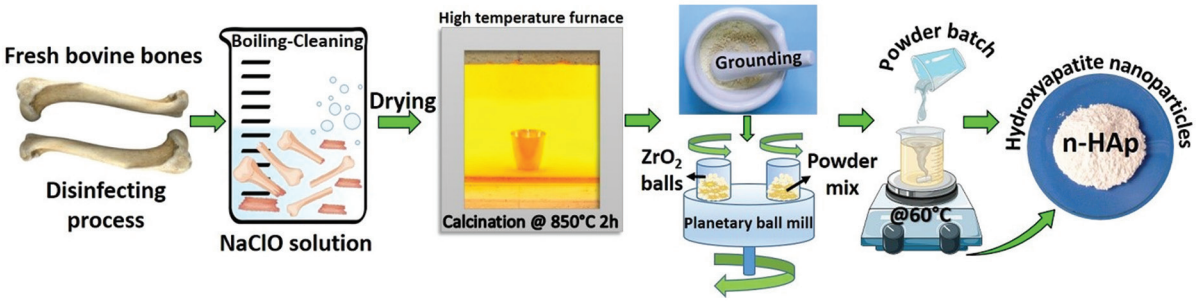

Figure 1. *The experimental steps for preparing n-HAp.*

Characterization of n-HAp by field emission scanning electron microscopy (FE-SEM), scanning transmission electron microscopy (S-TEM), and X-ray diffraction (XRD)

The microstructural analysis of n-HAp was conducted using field emission scanning electron microscopy (FE-SEM, Tescan Mira3 XMU, Brno, Czechia) to investigate particle morphology, shape, size, and phase formation. Before observation, the n-HAp samples were sputter-coated with gold for 2 min at 20 mA and then examined at an accelerating voltage of 10-20 kV. To further examine the detailed morphology of the resulting particle, S-TEM was employed. For S-TEM imaging on the FE-SEM, a transmission electron microscope (TEM) module was integrated onto the FE-SEM stage. The operating voltage utilized ranged from 15 to 30 kV, while the working distance was set to 3 mm to ensure a more precise evaluation of the sample on the Cu grid. The crystal structure analysis of the produced n-HAp was performed using an X-ray Diffractometer (Rigaku D/MAX/2200/PC) equipped with monochromatic Cu-K_α radiation (λ = 1.5408 Å). The instrument operated at an accelerating voltage of 40 kV and a current of 40 mA, and data were collected within a 2θ range spanning from 10° to 90°. To interpret the obtained data and characterize the crystal structure of the calcined and milled n-HAp, computer software (Jade; Materials Data Inc., Livermore, CA) was employed. By comparing the diffractograms with the standards provided by the joint committee of phase diffraction standards (JCPDS), a thorough analysis of the n-HAp crystal structure was achieved.

Cell culture analysis

In our cell culture experiments, we used L929 ATCC (NCTC clone 929@CCL-1) cells. These cells were grown in DMEM medium containing 10% FBS and 1% penicillin-streptomycin at 37°C with 95% humidity and 5% CO_2 in an incubator. The hydrogels were dissolved in 1 mL DMEM by stirring for 24 h at room temperature (150 rpm). We applied VG/nHAp gel to the cells at different concentrations (1%, 2.5%, 5%, and 10%). Cell viability (%) was calculated and plotted.[19].

Experimental animal analysis

For this research project, we used female Wistar albino rats (n = 60) that were newly adult, 16 weeks old, and not bred. The animals were housed under controlled laboratory conditions, including temperature, humidity, and a light–dark cycle. All experimental procedures conducted in this study were reviewed and approved by our university's Animal Research Ethics Committee under permit number 65202830-050.04.04-479. The care and handling of animals adhered to the European Communities Council Directive (86/609/EEC) for the protection of animals used for experimental purposes.

Vaginal injury model

A total of 60 rats were assigned randomly to four independent groups: Control Group (Control): No intervention. Laceration Group (SAM): Vaginal lacerations were induced. VG Group: VG was applied to the wound area. VG/nHAp Group: VG containing hydroxyapatite (n-HAp) was applied to the wound area. Each group was divided into 7th, 14th, and 21st day groups among themselves. There were 15 rats in the subgroups. All rats were fasted for 12 h before surgery. Animals were anesthetized with 2.5% isoflurane and placed on a heated table to maintain a body temperature of 37°C. After anesthesia was established, an 8-mm midline incision was performed in the posterior

vaginal wall, included the epitelial and posterior vaginal fibromuscular layers, sparing the anal sphincter and rectum.[20,21]. Postoperatively, the rats were monitored daily for signs of infection. Wounds were left to heal spontaneously in the sham group. In VG and VG/nHAp groups, bioadhesive gels were applied daily for 7, 14, and 21 days. The rats were housed in ventilated rooms and allowed to eat and drink ad libitum after surgery. The animals were sacrificed 7, 14, and 21 days after implantation samples were collected for biochemical and histological examinations. No antibiotic prophylaxes were administered, and no mortality occurred during the experiment. All surgical procedures were performed by the same surgeon under the same experimental conditions.

Biochemical analyses

In this study, on the 7th, 14th, and 21st days, blood samples were collected from all animals through intracardiac puncture into EDTA tubes. After centrifugation at 3000 rpm for 15 min, the serum was separated. Biochemical tests, including tumor necrosis factor alpha (TNF-α) (Cat No: E-EL-R2856, Elabscience), interleukin (IL)-1 (Cat No: E-EL-R0012, Elabscience), and vascular endothelial growth factor (VEGF) (Cat No: E-EL-R2603, Elabscience), were performed on the collected serum samples using the enzyme-linked immunosorbent assay (ELISA) method following the manufacturer's guidelines.

Histochemical analysis

The vaginal tissues obtained were fixed with 10% neutral buffered formalin. After fixation, the tissues were processed for tissue tracking and then embedded in paraffin. 4-5 μm-thick sections were obtained from the paraffin blocks using a Leica microtome[21]. The sections were stained with Hematoxylin and Eosin to assess epithelialization in the vaginal wound, inflammation in the lamina propria, and the amount of granulation tissue. In addition, Masson's trichrome staining (Masson's trichrome with aniline blue) was used to determine collagen fiber content, and the Silver impregnation technique was employed to assess reticular fiber content. The stained preparations were examined and photographed under a microscope (Olympus BX51, Japan). All histological examinations were conducted at the Department of Histology and Embryology, Faculty of Medicine, Sivas Cumhuriyet University. A blinded histologist evaluated the differences between groups based on tissue type and duration of injury. The main histological outcomes included the amount of inflammatory infiltration, granulation tissue, accumulation of collagen and reticular fibers, re-epithelialization, and neovascularization. These parameters represent the average values of five different histological images taken from vaginal tissue samples in each group. In this study, we used the histological scoring system proposed by Greenhalgh et al.[22] and Abramov et al.[2], as shown in table 1, with each parameter scored on a scale of 0-3.

Table 1. Wound-healing histologic scoring system (22, 2)

Variable	Score			
	0	1	2	3
Inflammation	None	Scant	Moderate	Abundant
Granulation tissue amount	None	Scant	Moderate	Abundant
Collagen deposition	None	Scant	Moderate	Abundant
Reticular fiber deposition	None	Scant	Moderate	Abundant
Re-epitelization	None	Partial	Complete but immature or thin	Complete and mature
Neovascularization	None	Up to five vessels per HPF	6-0 vessels/ HPF	More than 10 vessels per HPF

HPF: high-power field.

Statistical analysis

The mean values of biochemical data were calculated and plotted with ± SD using SigmaPlot 15.0. The two-tailed Friedman test was used for repeated measurements, and the Kruskal-Wallis test was used for comparison of independent groups. $p < 0.05$ was considered statistically significant. The Friedman test is a non-parametric alternative to one-way analysis of variance with repeated measures. It is used to test differences between groups when the dependent variable being measured is ordinal.

In the experimental vaginal wound model, vaginal healing criteria were scored according to table 1 and Friedman test was used to test whether there was a statistical difference between the scores obtained on the 7th, 14th, and 21st days for all variables in each

group and the significance level was set as α = 0.05. Another hypothesis of the study was whether there was a significant difference between the semi-quantitative score values on the 7th, 14th, and 21st day between the groups for each vaginal wound healing parameter. In order to test this hypothesis, the Kruskal-Wallis test, a non-parametric test, was applied at α = 0.05 significance level, and the results were obtained using the Statistical Package for the Social Sciences 25 statistical package program.

Results

Microstructural evolution of bone fragments and n-HAp

High-resolution FE-SEM photographs of bone fragments subjected to calcination, FE-SEM photographs of n-HAp obtained after calcination and ball milling of bone fragments, and S-TEM photographs taken for a more detailed examination of n-HAp are provided in figure 2.

When examining the FE-SEM photograph is shown in figure 2A, the morphology of the calcined bone pieces, which become quite fragile and brittle after the calcination process, is evident. In figure 2A, it was determined that after the applied calcination process, organic substances were effectively eliminated from the bone structure, and a distinct pore structure was formed with an average size of approximately 316 ± 130.25 μm.

From the microstructure photograph of the prepared n-HAp in figure 2B, it was observed that the structure, distributed in a uniform and homogeneous manner, consisted of a single phase. This homogeneity in morphology was noted as a positive physical feature in terms of high density and high performance. From the FE-SEM photographs, by counting at least 50 particles with distinct grain boundaries using the Image J analysis software program[23], the particle size of n-HAp was calculated to be approximately 460 ± 156 nm. In general, it was determined that the obtained n-HAps were irregularly shaped and partially in hemispherical form.

In the S-TEM analyses performed to visualize the n-HA crystals in more detail, the prepared powders were dispersed in isopropyl alcohol and passed through 200 nm filters[24]. After this process, large particles in the structure were removed from the environment, and S-TEM analyses were conducted. In the detailed photograph is shown in figure 2C, it was observed that the particles were below 500 nm in size and tended to aggregate. It was determined from the analysis that long-term grinding of n-HAp increased this phenomenon and resulted in particles with a high surface area.

Phase evolution of n-HAp by XRD analyses

Figure 2D displays the XRD patterns of n-HAp. The dominant crystal phase identified in the XRD patterns is hydroxyapatite (HAp) – $[Ca_5(PO_4)_3(OH)]$ with varying peak intensities. In all analyses, the diffractograms confirm the presence of $[Ca_5(PO_4)_3(OH)]$, which predominantly matches n-HAp (JCPDS card number 84-1998).

However, in the XRD results, in addition to the main phase, a small amount of minor β-tricalciumphosphate (TCP) (JCPDS card number 09-0169) peaks were detected. These small TCP peaks indicate the presence of β-TCP as a secondary phase next to the main HA phase in n-HAp. The β-TCP phase is a result of the decomposition of the HA mineral and represents stable polymorphs of the TCP mineral at various temperatures[25]. In the context of tissue engineering applications, when used/applied as a scaffold or filler, β-TCP is known to have significant potential in facilitating tissue regeneration, promoting angiogenesis (formation of new blood vessels), and increasing cell proliferation in both soft and hard tissues[26]. β-TCP is likely to play an increasingly important role in the development of medical therapies and treatments to improve patient outcomes and quality of life. X-ray analyses confirm the successful production of n-HAp as a filler nanoparticle for bioadhesive VGs (Fig. 2).

Cytotoxicity analysis

We applied VG/nHAp gel to the cells at different concentrations (1%, 2.5%, 5%, and 10%). Cell viability was calculated and plotted in figure 2. VG/nHAp applied on healthy L929 fibroblast cells did not result in significant differences in cell viability at different concentrations. VG/nHAp applied on healthy L929 fibroblast cells did not alter the nuclear morphology of cells at different concentrations (Fig. 3).

Biochemical analysis

In our experimental study, IL-1β, TNF-α, and VEGF levels in blood samples taken from all groups on days

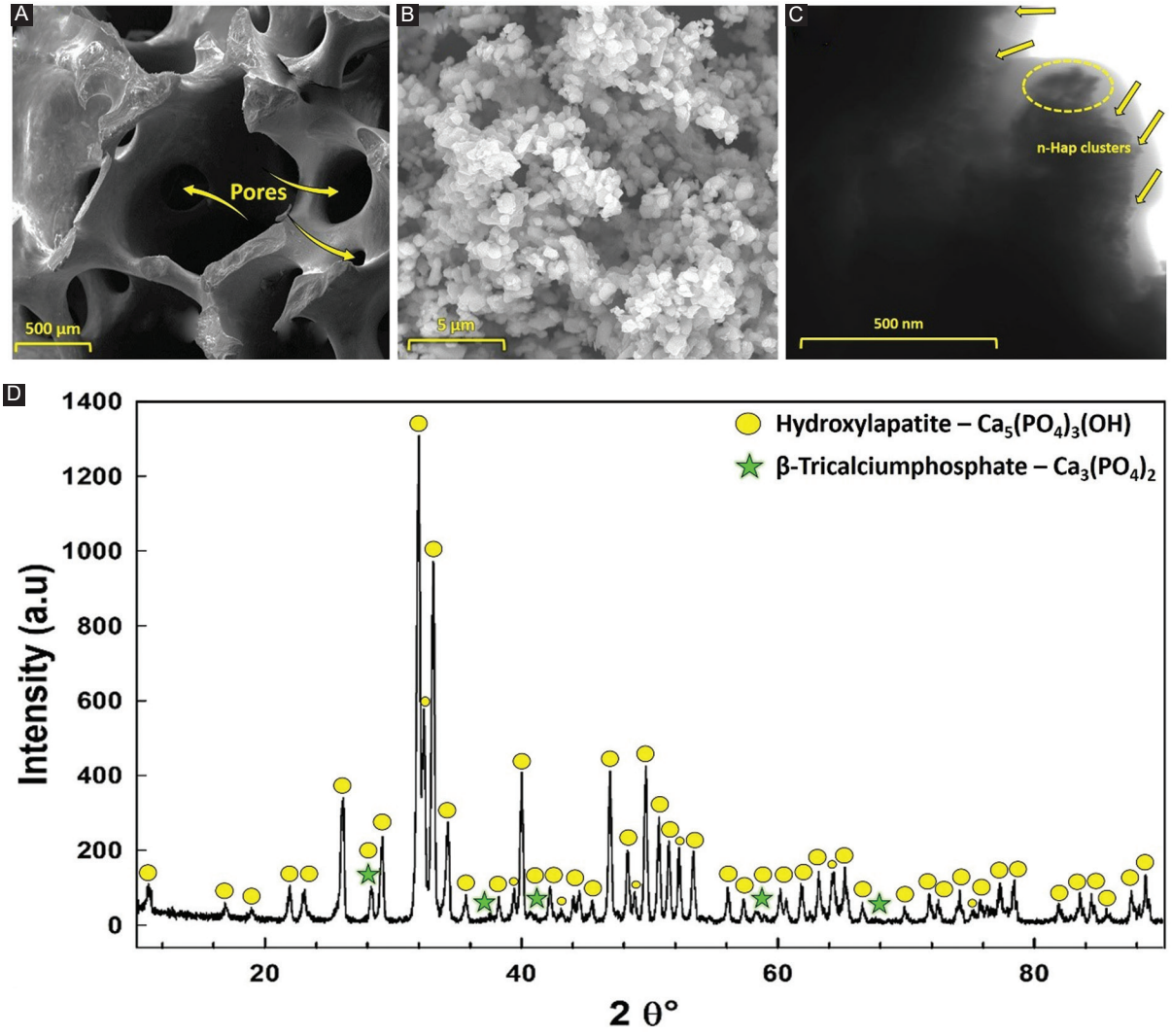

Figure 2. A: *high-resolution field emission scanning electron microscopy (FE-SEM) photographs of femoral bone fragments,* **B:** *after calcination at 850°C for 2 h,* **C:** *FE-SEM photographs of n-HAp after ball milling, and* **D:** *the X-ray diffraction patterns of the n-HAp.*

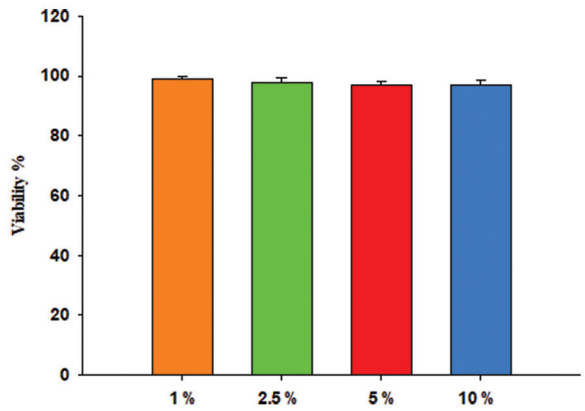

Figure 3. *Cell viability (%) results of vaginal gel/nHAp gel on L929 cell line at different concentrations.*

7, 14, and 21 were analyzed by the ELISA method. IL-1β and TNF-α, which are proinflammatory cytokines, regulate the mechanism by upregulating in the inflammatory phase of the wound healing process. IL-1β, TNF-α, and VEGF levels gradually decreased in Control, Sham, VG, and/nHAp groups on days 7, 14, and 21. However, as seen in Fig. 4A-C, this decrease is especially evident in the VG/nHAp group.

Histological analysis

On the 7th, 14th, and 21st days of the experiment, the typical multilayered squamous keratinized epithelium

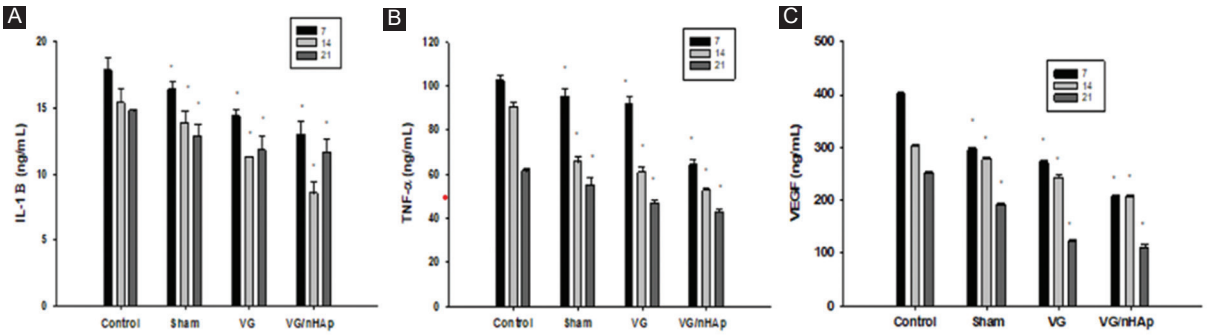

Figure 4. *Interleukin (IL)-1β, tumor necrosis factor alpha (TNF-α), VEGF enzyme-linked immunosorbent assay analysis values in blood serum samples obtained from Control, Sham, vaginal gel (VG), VG/nHAp groups on days 7, 14 and 21. According to the* **A:** *Kruskal-Wallis test IL-1β $p < 0.020$,* **B:** *Kruskal-Wallis test TNF-α $p < 0.023$,* **C:** *Kruskal-Wallis VEGF $p < 0.022$ were found when the control and all groups were compared pairwise. $p < 0.05$ was considered significant.*

of the vagina and the typical vaginal mucosa with many transverse folds together with the lamina propria located under it were evident in the control group (Fig. 5A). The basement membrane underlying the epithelium was thick and continuous, and collagen and reticular fibers were regularly arranged in the connective tissue forming the lamina propria (Fig. 5B and C). On the 7th day of the experiment, the number of epithelial layers, keratinization, and mucosal folds decreased, the number of inflammatory cells in the lamina propria increased, the number of collagen and reticular fibers decreased and became irregular in the Sham, VG, VG/nHAp groups compared to the control group. Newly formed blood vessels were significantly increased in the VG/nHAp group on the 7th day of the experiment. In the sham group, the epithelium was irregularly formed in the lamina propria, there were intense inflammatory cells, and collagen and reticular fibers were thin and irregularly arranged. Especially in the VG and VG/nHAp groups, the arrangement of connective tissue fibers in the tunica mucosa increased from the 7th day to the 14th and 21st days and markedly improved (Fig. 5A-C).

On the 7th, 14th, and 21st days of the experiment, the typical multilayered squamous keratinized epithelium of the vagina and the typical vaginal mucosa with many transverse folds with the lamina propria located underneath were evident in the control group (Fig. 5A). The basement membrane in which the epithelium was located was thick and continuous, while collagen and reticular fibers were regularly arranged in the connective tissue forming the lamina propria (Fig. 5B and C). On the 7th day of the experiment, the number of epithelial layers, keratinization, and mucosal folds decreased, the number of inflammatory cells in the lamina propria increased, the number of collagen and reticular fibers decreased and became irregular in the Sham, VG, VG/nHAp groups compared to the control group. Newly formed blood vessels were significantly increased in the VG/nHAp group on the 7th day of the experiment. In the sham group, the epithelium was irregularly formed in the lamina propria, there were intense inflammatory cells, and thin and irregularly arranged collagen and reticular fibers were remarkable. Especially in the VG and VG/nHAp groups, the arrangement of connective tissue fibers in the tunica mucosa increased from the 7th day to the 14th and 21st days and markedly improved (Fig. 5 A-C).

According to table 2, for the score values obtained from the subjects in the control group, no significant difference was found between the 7th, 14th, and 21st day scores in any parameter ($p > 0.05$). For the score values obtained from the subjects in the sham group, no significant difference was found between the 7th, 14th, and 21st day scores of the other parameters, except for the reepithelialisation parameter ($p > 0.05$). There was a significant difference for the re-epithelialization parameter ($p < 0.05$), and significant increases were observed at each follow-up time. Re-epithelialization value reached its highest value on the 21st day. For the score values obtained from the subjects in the VG group, no significant difference was found between the 7th, 14th, and 21st day scores of the other parameters, except for the inflammation parameter ($p > 0.05$). There was a significant difference for the inflammation parameter ($p < 0.05$), and significant decreases were observed at each follow-up time. Re-epithelialization value reached its lowest value at day 21. For the score values obtained from the subjects in the VG/nHAp group, a significant difference was found between the

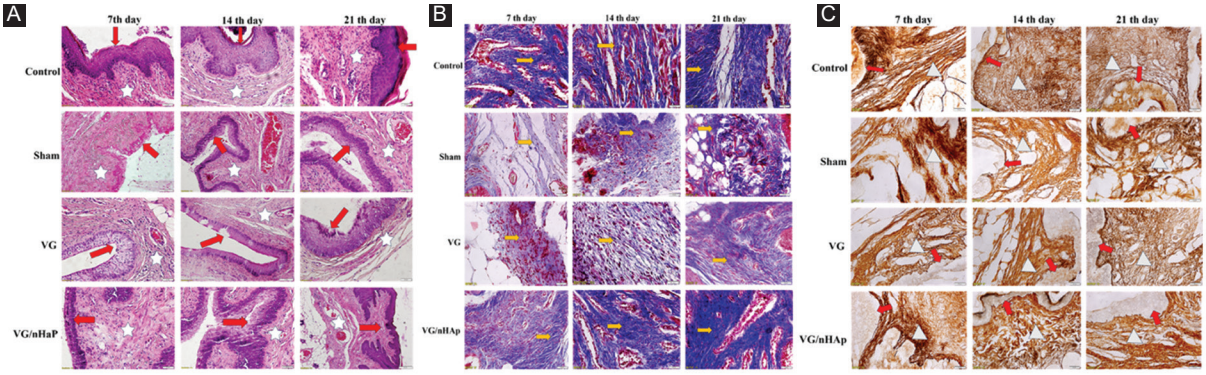

Figure 5. *Microscopic images obtained by staining with hematoxylin eosin (***A***), masson trichrome (***B***) and silver precipitation method (***C***) on paraffin tissue sections on the 7th, 14th, and 21st days in Control, Sham (wound created but no bioadhesive gel applied), VG (vaginal gel applied), and VG/nHAp (vaginal gel with nano hydroxyapatite particles) groups in which vaginal wound healing model was created.* **A:** *Microscopic photograph showing differences in epithelialization (arrow) and inflammation and neovascularization in the lamina propria (star) among Control, Sham, VG, and VG/nHAp groups on days 7, 14, and 21 in an experimental vaginal wound model (x20 Magnification, Hematoxylin and Eosin stain).* **B:** *Microscopic photograph shows differences in collagen fiber distribution (yellow arrows) among Control, Sham, VG, and VG/nHAp groups on days 7, 14, and 21 in an experimental vaginal wound model (x40 Magnification, MT stain).* **C:** *Microscopic photograph shows differences in reticular fiber distribution (white triangles) within the lamina propria (red arrow) beneath the epithelium among Control, Sham, VG, and VG/nHAp groups on days 7, 14, and 21 in an experimental vaginal wound model (x40 Magnification, Silver Imp).*

7th, 14th, and 21st day scores of the other parameters, except for collagen deposit and re-epithelialization parameters ($p < 0.05$). Although there were not enough changes to find a significant difference for re-epithelialization and collagen deposit parameters, increases were observed at follow-up times. For other parameters, significant differences were found between follow-up times and score values ($p < 0.05$). For the parameters of inflammation, granulation tissue amount, and neovascularization, significant decreases were observed at follow-up times, while the lowest values were reached on day 21. Significant increases were observed for the reticular deposit parameter at follow-up times and reached their highest value on the 21st day. The distribution of semi-quantitative score data for vaginal wound healing criteria obtained from the Control, Sham, VG, and n-HAp groups on days 7, 14, and 21 is shown in figure 6A.

According to the Kruskal-Wallis test results, a significant difference was found between the score values obtained on the 7th, 14th, and 21st days in terms of inflammation ($p < 0.05$). The mean ranks of inflammation, granulation, collagen and reticular fiber density, re-epithelialization and neovascularization score values of the subjects in the VG/nHAp group were found to be significantly different in the VG/nHAp group compared to the control group in accordance with the wound healing stages ($p < 0.05$) (Table 3). The distribution of semi-quantitative score data for vaginal wound healing criteria obtained on days 7, 14, and 21 according to the control, sham, VG, and VG/nHAp groups is shown in figure 6B.

Discussion

Surgical incision to the perineum, such as episiotomy, is known to cause various problems on vaginal wound healing. Although different methods have been proposed to reduce the rate of perineal laceration, an effective method has not yet been found due to the complications experienced afterward[27].

In today's biomedical applications, various natural polymer-based gels, hydrogels, and porous scaffolds have significant potential to simultaneously fulfill expected properties[28-30]. Sodium Alginate (SA), an anionic linear polysaccharide composed of 1,4-linked β-D-mannuronic acid (M) and α-L-guluronic acid (G) residues, holds promise due to its good biocompatibility, biodegradability, non-toxicity, and non-immunogenicity. It has been recognized as a valuable biopolymer[31-33]. Carboxymethyl cellulose (CMC), another natural polymeric biomaterial similar to SA, has been shown to support the stability of cellular environments *in vivo* and promote increased cell viability over time.

Various polymers with bioadhesive properties have been reported in the literature[34,35], including polyacrylates (polycarbophil and carbomer), cellulosic derivatives (sodium carboxymethylcellulose, hydroxypropylmethylcellulose, and hydroxyethylcellulose), and other

Table 2. Friedman test table for semi quantitative score data of vaginal wound healing criteria obtained from Control, Sham, VG, VG/nHAp groups on the 7th, 14th, and 21st days

Groups	Parameters	Days	Mean	Standard deviation	Minimum	Maximum	Mean rank	p
Control	Inflammation	7	0.2	0.447	0	1	2.20	0.368
		14	0	0.000	0	0	1.90	
		21	0	0.000	0	0	1.90	
	Granulation tissue amount	7	0	0.000	0	0	2.00	1.000
		14	0	0.000	0	0	2.00	
		21	0	0.000	0	0	2.00	
	Collagen deposit	7	3	0.000	3	3	2.00	1.000
		14	3	0.000	3	3	2.00	
		21	3	0.000	3	3	2.00	
	Reticular deposit	7	2.8	0.447	2	3	1.80	0.368
		14	3	0.000	3	3	2.10	
		21	3	0.000	3	3	2.10	
	Re-epithelization	7	3	0	3	3	2.00	1.000
		14	3	0	3	3	2.00	
		21	3	0	3	3	2.00	
	Neovascularization	7	2	0	2	2	1.90	0.368
		14	2.2	0.447	2	3	2.20	
		21	2	0	2	2	1.90	
Sham	Inflammation	7	2.8	0.447	2	3	2.30	0.444
		14	2.6	0.548	2	3	2.10	
		21	2.2	0.837	1	3	1.60	
	Granulation tissue amount	7	1.8	0.837	1	3	2.30	0.165
		14	1.8	0.447	1	2	2.30	
		21	1.2	0.447	1	2	1.40	
	Collagen deposit	7	1.2	0.447	1	2	1.50	0.082
		14	1.6	0.548	1	2	2.00	
		21	2	1.000	1	3	2.50	
	Reticular deposit	7	1	0.707	0	2	1.50	0.210
		14	1.4	0.548	1	2	2.00	
		21	2	0.707	1	3	2.50	
	Re-epithelization	7	0.4	0.548	0	1	1.30	0.037*
		14	1	0.707	0	2	2.10	
		21	1.6	0.548	1	2	2.60	
	Neovascularization	7	1.8	0.837	1	3	2.50	0.174
		14	1.2	0.447	1	2	1.90	
		21	1	0.000	1	1	1.60	

(Continues)

Table 2. Friedman test table for semi quantitative score data of vaginal wound healing criteria obtained from Control, Sham, VG, VG/nHAp groups on the 7th, 14th, and 21st days *(continued)*

Groups	Parameters	Days	Mean	Standard deviation	Minimum	Maximum	Mean rank	p
VG	Inflammation	7	2.4	0.548	2	3	2.70	0.039*
		14	1.8	0.837	1	3	1.80	
		21	1.6	0.548	1	2	1.50	
	Granulation tissue amount	7	2.2	0.447	2	3	2.40	0.273
		14	1.8	0.447	1	2	1.90	
		21	1.6	0.548	1	2	1.70	
	Collagen deposit	7	1.6	0.548	1	2	1.60	0.202
		14	2	0.707	1	3	2.00	
		21	2.4	0.548	2	3	2.40	
	Reticular deposit	7	1.2	0.447	1	2	1.50	0.074
		14	1.4	0.548	1	2	1.80	
		21	2.2	0.447	2	3	2.70	
	Re-epithelization	7	1.2	0.837	0	2	1.50	0.109
		14	1.8	0.447	1	2	1.90	
		21	2.4	0.548	2	3	2.60	
	Neovascularization	7	2	0.707	1	3	1.90	0.607
		14	2.2	0.447	2	3	2.20	
		21	2	0.707	1	3	1.90	
VG/nHAp	Inflammation	7	1.6	0.548	1	2	2.70	0.037*
		14	1	0.707	0	2	1.90	
		21	0.6	0.548	0	1	1.40	
	Granulation tissue amount	7	2.8	0.447	2	3	2.80	0.039*
		14	1.8	0.837	1	3	1.80	
		21	1.2	0.837	0	2	1.40	
	Collagen deposit	7	2.2	0.447	2	3	1.50	0.074
		14	2.4	0.548	2	3	1.80	
		21	3	0.000	3	3	2.70	
	Reticuler deposit	7	1.8	0.447	1	2	1.40	0.048*
		14	2.2	0.447	2	3	2.00	
		21	2.6	0.548	2	3	2.60	
	Reepitelization	7	2.2	0.837	1	3	1.50	0.082
		14	2.6	0.548	2	3	2.00	
		21	3	0.000	3	3	2.50	
	Neovascularization	7	3	0.000	3	3	2.90	0.015*
		14	2.2	0.447	2	3	1.80	
		21	1.6	0.548	1	2	1.30	

* indicates a statistically significant difference at $p < 0.05$, VG: vaginal gel.

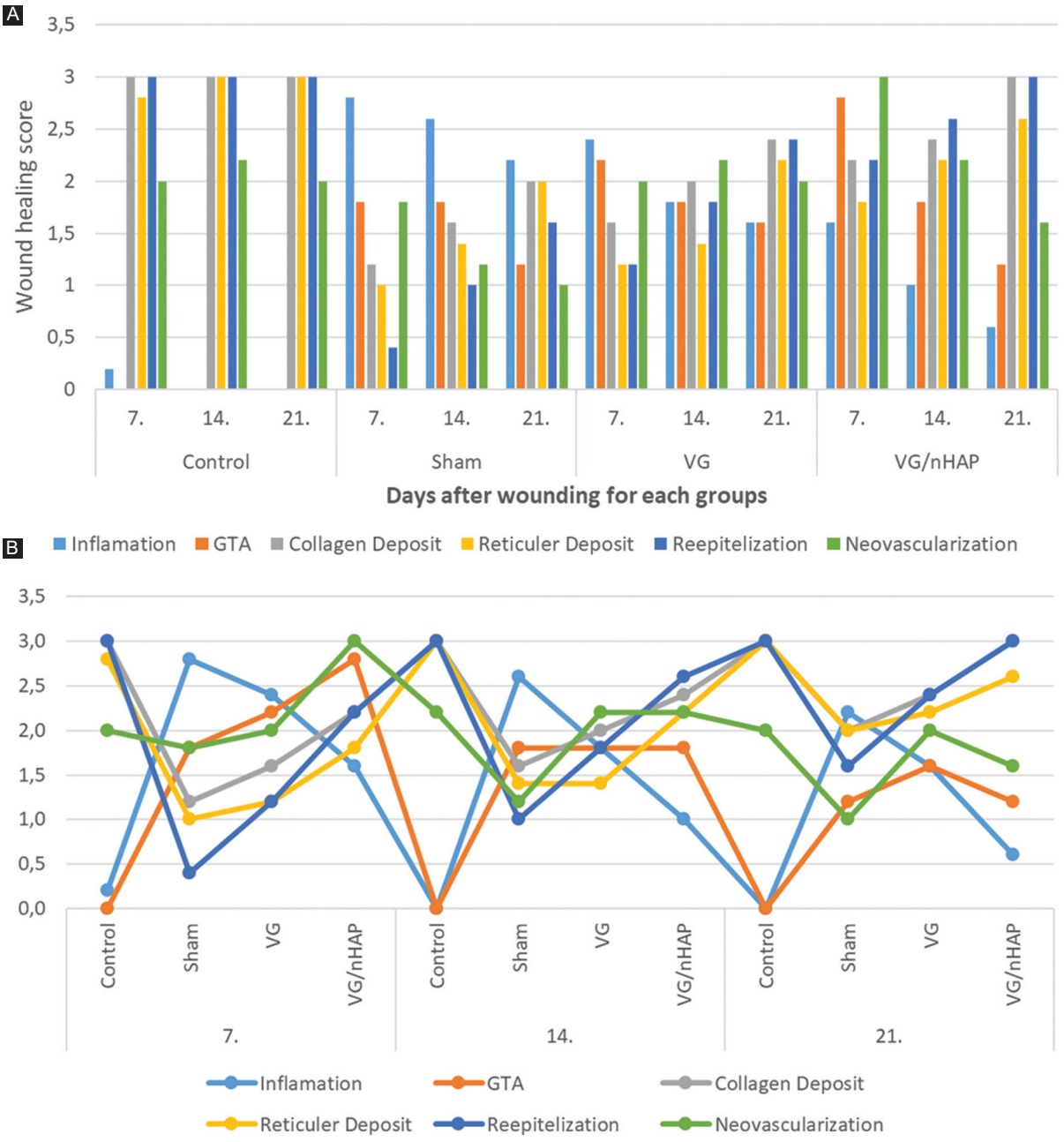

Figure 6. A: *Friedman test graph of semi quantitative score data of vaginal wound healing criteria obtained from Control, Sham, Vaginal gel (VG), n-HAp groups at 7, 14, and 21 days.* **B:** *Kruskal-Wallis test graph of semi quantitative score data of vaginal wound healing criteria obtained from Control, Sham, VG, VG/nHAp groups at 7, 14, and 21 days.*

polysaccharides (chitosan, hyaluronic acid, and gums). Among the limited number of polymer combinations studied for commercial muco-adhesive drug delivery systems, most vaginal semi-solid products are based on cellulosic and polyacrylic polymers[36,37]. Therefore, further research is needed on the application of different combinations of biodegradable biopolymers for bioadhesive VGs. In this study, it was observed that the synthesized polymer combinations increased the biological adhesive properties, and simultaneously, the addition of bioactive n-HAp enhanced the stability of the gels. Polymeric structures designed as biomaterials are among the most suitable options for mimicking the main structure of soft tissues. However, the incorporation of different additives into the polymer matrix can accelerate the development of biological properties and wound healing processes.

Table 3. Kruskal-Wallis analysis table of semi quantitative score data of vaginal wound healing criteria obtained from control, sham, VG, VG/nHAp groups on the 7th, 14th, and 21st days

Inflammation					Granulation tissue amount				
Days	**Groups**	**n**	**Mean rank**	**p**	**Days**	**Groups**	**n**	**Mean rank**	**p**
7	Control	5	3.2	0.002	7	Control	5	3	0.002
	Sham	5	16.2			Sham	5	10.5	
	VG	5	13.6			VG	5	12.3	
	VG/nHAp	5	9			VG/nHAp	5	16.2	
14	Control	5	3.5	0.002	14	Control	5	3	0.006
	Sham	5	16.7			Sham	5	13.1	
	VG	5	12.9			VG	5	13.1	
	VG/nHAp	5	8.9			VG/nHAp	5	12.8	
21	Control	5	4	0.002	21	Control	5	3.5	0.01
	Sham	5	16.3			Sham	5	11.9	
	VG	5	13.8			VG	5	14.7	
	VG/nHAp	5	7.9			VG/nHAp	5	11.9	
Collagen deposit					**Reticular deposit**				
Days	**Groups**	**n**	**Mean rank**	**p**	**Days**	**Groups**	**n**	**Mean rank**	**p**
7	Control	5	17.5	0.002	7	Control	5	17.4	0.005
	Sham	5	4.9			Sham	5	6.1	
	VG	5	7.7			VG	5	7	
	VG/nHAp	5	11.9			n-HAp	5	11.5	
14	Control	5	16.5	0.012	14	Control	5	17.5	0.003
	Sham	5	5.6			Sham	5	6.3	
	VG	5	8.5			VG	5	6.3	
	n-HAp	5	11.4			n-HAp	5	11.9	
21	Control	5	13.5	0.044	21	Control	5	15.5	0.039
	Sham	5	6.9			Sham	5	6.9	
	VG	5	8.1			VG	5	7.9	
	VG/nHAp	5	13.5			VG/nHAp	5	11.7	
Reepitelization					**Neovascularization**				
Days	**Groups**	**n**	**Mean Rank**	**p**	**Days**	**Groups**	**n**	**Mean Rank**	**p**
7	Control	5	17	0.003	7	Control	5	8.5	0.02
	Sham	5	4.3			Sham	5	7.6	
	VG	5	7.9			VG	5	8.9	
	VG/nHAp	5	12.8			VG/nHAp	5	17	

(Continues)

Table 3. Kruskal-Wallis analysis table of semi quantitative score data of vaginal wound healing criteria obtained from control, sham, VG, VG/nHAp groups on the 7th, 14th, and 21st days *(continued)*

Inflammation					Granulation tissue amount				
Days	**Groups**	**n**	**Mean rank**	**p**	**Days**	**Groups**	**n**	**Mean rank**	**p**
14	Control	5	16.5	0.002	14	Control	5	12.6	0.014
	Sham	5	4.1			Sham	5	4.2	
	VG	5	7.9			VG	5	12.6	
	VG/nHAp	5	13.5			VG/nHAp	5	12.6	
21	Control	5	14.5	0.002	21	Control	5	14	0.015
	Sham	5	3.9			Sham	5	4.5	
	VG	5	9.1			VG	5	13.3	
	VG/nHAp	5	14.5			VG/nHAp	5	10.2	

VG: vaginal gel.

Among these additives, bioceramics such as bioglasses, carbon nanostructures, and HAp, which contribute to tissue healing, can be preferred for applications in both hard and soft tissues[38,39]. HAp, one of the bioceramics used in tissue healing, offers fundamental benefits to tissues such as promoting cell growth and proliferation, inducing angiogenesis, and possessing antimicrobial properties[40]. n-HAp also enhances fibroblast activity in injured areas and contributes to wound dressing/burn treatment when incorporated into various soft organic matrices to improve the mechanical properties and thermal stability of the polymer[41]. Therefore, the use of HA microparticles (size < 74 μm) in combination with gels at skin wound sites further enhances fibroblast maturation and re-epithelialization due to the beneficial effects of the ion-charged stored in the gel[42].

The purpose of biocompatibility testing is to determine the suitability of a substance for human use and to see whether it has potentially harmful physiological effects. *In vitro* and in *vivo* studies are performed in biocompatibility tests. Therefore, we performed biocompatibility tests *in vitro* in our study (ISO/EN10993-5). Possible vaginal wound healing material (VG/nHAp) was prepared in four different concentrations and was observed to be non-toxic. In addition, the material did not change the proliferation and morphology of healthy cells. In the study conducted by Malafaya and Reis[43], the toxicity of HAp produced was evaluated in the L929 healthy fibroblast cell line, and it was stated that it was not toxic.

The steps of wound repair in skin and vaginal tissue have common similarities. Compared to skin healing, the proliferation and migration of local vaginal fibroblasts is coordinated with local vaginal epithelial cells at the wound edges to ensure granulation tissue formation and re-epithelialization during the vaginal wound healing process. For example, a scab does not form during vaginal wound healing as in dermal wounds. After injury in dermal tissues, a clot is formed, and inflammatory cells enter the injured tissue, and abundant leukocytes and plasma proteins migrate to the healing area. Initially, neutrophils arrive, sterilize, and debride the wound. Monocytes and tissue macrophages dominate the inflammatory response within 2-3 days. After the initial inflammatory response, inflammation continues with a gradual disappearance of inflammatory cells. Inflammation is intensely observed in the first 7 days of wound healing and gradually decreases[44]. In our study, on the 7th day of vaginal injury, more intense inflammation was observed in the Sham group than in the VG and VG/nHAp groups, while it decreased on the 14th and 21st days. Less inflammation was determined in the VG and VG/nHAp groups compared to the Sham group. The VG/nHAp group had the least number of inflammatory cells.

Cytokines and growth factors, which are protein molecules that provide communication between cells in the body, manage important processes after vaginal injury. Cytokines enable the migration of inflammatory cells and fibroblasts to the wound site during the wound healing phase, and organize the formation and production of extracellular matrix (ECM) by activating cell proliferation and angiogenesis. Both human and animal studies emphasize that high local and circulating TNF-α levels are associated with impaired wound healing. It has been suggested that treating women with TNF-α antagonists following vaginal surgeries may have a therapeutic effect, resulting in an improved wound healing process. However, macrophages are involved in both the inflammatory and proliferation phases of wound healing. TNF-α and IL-1β are proinflammatory cytokines secreted by M1 macrophages during the inflammatory phase. M2 macrophages release polyamines for the induction of VEGF expression and collagen production. If this polarization from M1 macrophages to M2 macrophages is disrupted, wound healing is impaired. This disruption slows the rate of re-epithelialization, granulation tissue formation, and vascularization[45]. Our study supports the literature. A decrease in TNF-α and VEGF values was observed in VG and VG/nHAp groups. There is a decrease in TNF-α and VEGF values in the VG/nHAp group, which shows that the fastest recovery is in this group.

In dermal tissues, fibroblasts have been reported to migrate into acute wounds within 2 days and become the main cell type of granulation tissue on day 4 post-injury. Fibroblasts fill the wound site through migration and increase in number by proliferation. These functions are accompanied by various growth factors. In addition to the behavior of fibroblasts, neovascularization also accompanies the repair process in the vaginal wound. Thus, granulation tissue forms in the vagina on the 4th day[46]. When we look at our study, granulation tissue in the Sham group gradually decreased from day 7 to day 21 because it represents normal vaginal healing. On the other hand, it was determined that the maturation process of granulation tissue in the VG and VG/nHAp groups matured faster than in the control on day 7, and the rate of granulation tissue formation in the VG/nHAp group was higher than the VG group.

Neovascularization is an important component of the wound healing process, involving the branching and expansion of adjacent blood vessels as well as endothelial progenitor cells[47]. In the control group, it was determined that neovascular structures decreased from the 7th day until the 21st day. In the VG and VG/nHAp groups used in the vaginal healing model, neovascular structures increased much more significantly from day 7. New vessel formation was observed more prominently in the VG/nHAp group as of day 7. During wound healing in the skin, fibroblasts have been shown to accumulate increased amounts of fibrillar collagen, which is important for wound healing. This process is regulated by the same growth factors that regulate fibroblast proliferation.

It has been shown that collagen deposition by skin fibroblasts starts within 3-5 days after injury and continues for several weeks, depending on the size of the wound[48,49]. Type 1 and type 3 forms of collagen, which have various subtypes, are commonly found in skin and mucosa. They strongly bind to cells to support epithelial and lamina propria formation and maintain tissue integrity[50]. In our study, we wanted to determine the amount of collagen with masson trichrome stain and reticular fiber (type 3) collagen with the silver precipitation technique to understand whether wound healing occurs properly with the proposed biomaterials. In the sham group, the amount of collagen fiber increased from the 7th to the 21st day after injury.

However, the amount of collagen and reticular fiber in the VG and VG/nHAp groups was higher than in the Sham group. Especially in the VG/nHAP group, there was a significant increase in collagen and reticular fibers compared to the other groups.

The normal vaginal epithelium is moist and thick. The natural shedding of epithelial cells into the vagina leads to the release of glycogen, which is converted into lactic acid by lactobacilli to maintain the balance of the vagina. Epithelial cells are surrounded and supported by an abundant ECM, normally rich in type I and type III collagens. The amount of these two collagen proteins has a significant effect on the symptoms of vaginal injury. It is stated that collagen-based biomaterial application to rats with vaginal atrophy increases vaginal epithelial height and increases cell adhesion molecules and ECM markers[51]. It has been shown that re-epithelialization in dermal tissues occurs within 24-48 h after injury when the spurs of epithelial cells move from the wound edges along the cut edges of the dermis and accumulate basement membrane components supported by type 3 collagen. Eventually, they fused to form a continuous epithelial layer covering the wound. It is stated that wound re-epithelialization in the vagina starts in a short period of time and progresses similarly to that in the skin and is almost completed on days 14-21[2]. In our study, although it was determined that re-epithelialization was completed on the 21st day in the Sham group, epithelial elevation and keratinization did not occur. On the other hand, a significant difference was observed in the VG/nHAp group compared to the other groups as of day 14. In this group, the epithelium was closed, epithelial folds were completed, and mucosal folds became prominent on the 21st day.

Conclusion

The bioadhesive gel prepared with n-HAp was successfully synthesized. In the study, the characterization of the gel was determined by FE-SEM, S-TEM, and XRD. Images of the gel, which exhibited porous structures with optimal mechanical properties similar to bone, were confirmed by what was reported in the literature. After it was observed that the VG was not toxic, it was used in the *in vivo* experiment. In animal experiments, a wound was opened in the vagina of rats and bioadhesive gel was applied. As a result, bioadhesive gel prepared with HAp is seen as promising for the treatment of vaginal wounds. However, its safety and efficacy should be tested in the clinical setting, which is the next step for biocompatibility experiments, by conducting extensive research.

Funding

The authors declare that they have not received funding.

Conflicts of interest

The authors declare no conflicts of interest.

Ethical considerations

Protection of humans and animals. The authors declare that the procedures followed complied with the ethical standards of the responsible human experimentation committee and adhered to the World Medical Association and the Declaration of Helsinki. The procedures were approved by the institutional Ethics Committee.

Confidentiality, informed consent, and ethical approval. The study does not involve patient personal data nor requires ethical approval. The SAGER guidelines were followed according to the nature of the study.

Declaration on the use of artificial intelligence. The authors declare that no generative artificial intelligence was used in the writing of this manuscript.

References

1. Alperin M, Feola A, Meyn L, Duerr R, Abramowitch S, Moalli P. Collagen scaffold: a treatment for simulated maternal birth injury in the rat model. Am J Obstetr Gynecol. 2010;202:589.e1-8.
2. Abramov Y, Golden B, Sullivan M, Botros SM, Miller JJ, Alshahrour A, et al. Histologic characterization of vaginal vs. Abdominal surgical wound healing in a rabbit model. Wound Repair Regen. 2007;15:80-6.
3. Khajehei M, Swain J, King J, Compton C, Wei W, McGee T, et al. Optimising recovery after perineal trauma: implementation of an evidence-based patient-centred care and clinical practice guideline. Women Birth. 2024;37:101584.
4. Bal-Ozturk A, Cecen B, Avci-Adali M, Topkaya SN, Alarcin E, Yasayan G, et al. Tissue adhesives: from research to clinical translation. Nano Today. 2021;36:101049.
5. Gennari R, Rotmensz N, Ballardini B, Scevola S, Perego E, Zanini V, et al. A prospective, randomized, controlled clinical trial of tissue adhesive (2-octylcyanoacrylate) versus standard wound closure in breast surgery. Surgery. 2004;136:593-9.
6. Muglali M, Yılmaz N, Inal S, Guvenc T. Immunohistochemical comparison of indermil with traditional suture materials in dental surgery. J Craniofac Surg. 2011;22:1875-9.
7. Vokrri L, Qavdarbasha A, Rudari H, Ahmetaj H, Manxhuka-Kërliu S, Hyseni N, et al. Experimental study of sutureless vascular anastomosis with use of glued prosthesis in rabbits. Vasc Health Risk Manag. 2015;11:211-7.
8. Öksüz KE, Kilinç S, Özer A. Effect of calcination on microstructure development and properties of hydroxyapatite powders extracted from human and bovine bones. Trans Indian Ceram Soc. 2019;78:41-5.
9. Özer A, Öksüz KE. The effect of yttrium oxide in hydroxyapatite/aluminum oxide hybrid biocomposite materials: phase, mechanical and morphological evaluation. Materialwiss Werkstofftech. 2019;50:1382.

10. Gunduz O, Gode C, Ahmad Z, Gökçe H, Yetmez M, Kalkandelen C, et al. Preparation and evaluation of cerium oxide-bovine hydroxyapatite composites for biomedical engineering applications. J Mech Behav Biomed Mater. 2014;35:70-6.
11. Tosun GN, Ozer A, Bektas T, Oksuz KE, Tayhan SE, Ozdemir T. Silk sericin-hydroxyapatite nanoribbons toward structurally stable osteogenic scaffolds. J Aust Ceram Soc. 2023;59:1291-301.
12. Ensign LM, Cone R, Hanes J. Nanoparticle-based drug delivery to the vagina: a review. J Control Release. 2024;190:500-14.
13. Vanić E, Škalko-Basnet N. Nanopharmaceuticals for improved topical vaginal therapy: can they deliver? Eur J Pharm Sci. 2013;50:29-41.
14. Kurt B, Oksuz KE, Sahin-Inan ZD, Hepokur C. Efecto antiadhesivo de nanopartículas de dihidrato de fosfato dicálcico obtenidas naturalmente en el modelo de herida uterina de rata. Cir Cir. 2023;91:457-67.
15. Öksüz KE, Kurt B, Şahin-İnan ZD, Hepokur C. Novel bioactive glass/graphene oxide-coated surgical sutures for soft tissue regeneration. ACS Omega. 2023;8:21628-41.
16. Bohórquez-Moreno CD, Öksüz KE, Dinçer E, Hepokur C, Şen L. Plant-inspired adhesive and injectable natural hydrogels: *in vitro* and *in vivo* studies. Biotechnol Lett. 2023;45:1209-22.
17. Zhang M, Zhuang B, Du G, Han G, Jin Y. Curcumin solid dispersion-loaded *in situ* hydrogels for local treatment of injured vaginal bacterial infection and improvement of vaginal wound healing. J Pharm Pharmacol. 2019;71:1044-54.
18. Cottam E, Hukins DW, Lee K, Hewitt C, Jenkins MJ. Effect of sterilisation by gamma irradiation on the ability of polycaprolactone (PCL) to act as a scaffold material. Med Eng Phys. 2009;31:221-6.
19. Canciani E, Sirello R, Pellegrin G, Henin D, Perrotta M, Toma M, et al. Effects of vitamin and amino acid-enriched hyaluronic acid gel on the healing of oral mucosa: *in vivo* and *in vitro* study. Medicina (Kaunas). 2021;57:285.
20. Ben Menachem-Zidon O, Parkes I, Chill HH, Reubinoff B, Sandberg K, Ji H, et al. Age-associated differences in macrophage response in a vaginal wound healing rat model. Int Urogynecol J. 2020;31:1803-9.
21. Shveiky D, Iglesia CB, Sarkar-Das S, Ben Menachem-Zidon O, Chill H, Ji H, et al. Age-associated impairments in tissue strength and immune response in a rat vaginal injury model. Int Urogynecol J. 2020;31:1435-41.
22. Greenhalgh DG, Sprugel KH, Murray MJ, Ross R. PDGF and FGF stimulate wound healing in the genetically diabetic mouse. Am J Pathol. 1990;136:1235-46.
23. Bin Mobarak M, Hossain MS, Chowdhury F, Ahmed S. Synthesis and characterization of CuO nanoparticles utilizing waste fish scale and exploitation of XRD peak profile analysis for approximating the structural parameters. Arab J Chem. 2022;15:104117.
24. González-Martínez DA, González Ruíz G, Luzardo Lorenzo MC, Bordallo-León F, Hechavarría Luna Y, Cazañas Quintana Y, et al. Hydroxyapatite nanoparticles as a potential long-term treatment of cancer of epithelial origin. ACS Appl Nano Mater. 2022;5:6159-70.
25. Best SM, Porter AE, Thian ES, Huang J. Bioceramics: past, present and for the future. J Eur Ceram Soc. 2008;28:1319-27.
26. Bi G, Mo L, Li, S, Zhong X, Yang J, Yuan Z, et al. DLP printed β-tricalcium phosphate functionalized ceramic scaffolds promoted angiogenesis and osteogenesis in long bone defects. Ceram Int. 2022;48:26274-86.
27. Jiang H, Qian X, Carroli G, Garner P. Selective versus routine use of episiotomy for vaginal birth. Cochrane Database Syst Rev. 2017;2:CD00081.
28. Fernandez-Yague MA, Abbah SA, McNamara L, Zeugolis DI, Pandit A, Biggs MJ. Biomimetic approaches in bone tissue engineering: ıntegrating biological and physicomechanical strategies. Adv Drug Deliv Rev. 2015;84:1-29.
29. Sharma C, Dinda AK, Potdar PD, Chou CF, MishraNC. Fabrication and characterization of novel nano-biocomposite scaffold of chitosan-gelatin-alginate-hydroxyapatite for bone tissue engineering. Mater Sci Eng C Mater Biol Appl. 2016;64:416-27.
30. Bohorquez-Moreno CD, Öksüz KE, Dinçer E. Porous polymer scaffolds derived from bioresources for biomedical applications. Cellulose Chem Technol. 2023;57:107-16.
31. Sarker B, Li W, Zheng K, Detsch R, Boccaccini AR. Designing porous bone tissue engineering scaffolds with enhanced mechanical properties from composite hydrogels composed of modified alginate, gelatin, and bioactive glass. ACS Biomater Sci Eng. 2016;2:2240-54.
32. Venkatesan J, Bhatnagar I, Manivasagan P, Kang KH, Kim SK. Alginate composites for bone tissue engineering: a review. Int J Biol Macromol. 2015;72:269-81.
33. Kuo CK, Ma PX. Ionically crosslinked alginate hydrogels as scaffolds for tissue engineering: part 1. Structure, gelation rate and mechanical properties. Biomaterials. 2001;22:511-21.
34. Andrews GP, Laverty TP, Jones DS. Mucoadhesive polymeric platforms for controlled drug delivery. Eur J Pharm Biopharm. 2009;71:505-18.
35. Morales JO, McConville JT. Manufacture and characterization of mucoadhesive buccal films. Eur J Pharm Biopharm. 2011;77:187-99.
36. Das Neves J, Bahia MF. Gels as vaginal drug delivery systems. Int J Pharm. 2006;318:1-14.
37. Valenta C. The use of mucoadhesive polymers in vaginal delivery. Adv Drug Deliv Rev. 2005;57:1692-712.
38. Gorain B, Choudhury H, Pandey M, Kesharwani P, Abeer MM, Tekade RK, et al. Carbon nanotube scaffolds as emerging nanoplatform for myocardial tissue regeneration: a review of recent developments and therapeutic implications. Biomed Pharmacother. 2018;104:496-508.
39. Xu X, Liu X, Tan L, Cui Z, Yang X, Zhu S, et al. Controlled-temperature photothermal and oxidative bacteria killing and acceleration of wound healing by polydopamine-assisted au-hydroxyapatite nanorods. Acta Biomater. 2018;77:352-64.
40. Yu Q, Chang J, Wu C. Silicate bioceramics: from soft tissue regeneration to tumor therapy. J Mater Chem B. 2019;7:5449-60.
41. Türe H. Characterization of hydroxyapatite-containing alginate-gelatin composite films as a potential wound dressing. Int J Biol Macromol. 2019;123:878-88.
42. Okabayashi R, Nakamura M, Okabayashi T, Tanaka Y, Nagai A, Yamashita K. Efficacy of polarized hydroxyapatite and silk fibroin composite dressing gel on epidermal recovery from full‐thickness skin wounds. J Biomed Mater Res B Appl Biomater. 2009;90B:641-6.
43. Malafaya PB, Reis RL. Bilayered chitosan-based scaffolds for osteochondral tissue engineering: influence of hydroxyapatite on *in vitro* cytotoxicity and dynamic bioactivity studies in a specific double-chamber bioreactor. Acta Biomater. 2009;5:644-60.
44. Henry G, Garner WL. Inflammatory mediators in wound healing. Surg Clin North Am. 2003;83:483-507.
45. Kimball A, Schaller M, Joshi A, Davis FM, DenDekker A, Boniakowski A, et al. Ly6CHi blood monocyte/macrophage drive chronic inflammation and impair wound healing in diabetes mellitus. Arterioscler Thromb Vasc Biol. 2018;38:1102-14.
46. Paulsson Y, Hammacher A, Heldin CH, Westermark B. Possible positive autocrine feedback in the prereplicative phase of human fibroblasts. Nature. 1987;328:715-7.
47. Carmeliet P. Angiogenesis in health and disease. Nature Med. 2003;9(6):653-60.
48. Cohen IK, Die-Gelmann RF, Lindblad WJ, Hugo NE. Wound healing: biochemical and clinical aspects. Plast Reconstr Surg. 1992;90:926.
49. O'Kane S. Wound remodelling and scarring. J Wound Care. 2002;11: 296-9.
50. Li H, Duann P, Lin PH, Zhao L, Fan Z, Tan T, et al. Modulation of wound healing and scar formation by MG53 protein-mediated cell membrane repair. J Biol Chem. 2015;290:24592-603.
51. You S, Liu S, Dong X, Li H, Zhu Y, Hu L. Intravaginal administration of human type III collagen-derived biomaterial with high cell-adhesion activity to treat vaginal atrophy in rats. ACS Biomater Sci Eng. 2020;6: 1977-88.